# Condensation of Mixed Vapors and Thermodynamics

**Srinivas R. Vuddagiri and Philip T. Eubank**
Dept. of Chemical Engineering, Texas A&M University, College Station, TX 77843

*A literal interface between thermodynamics and transport phenomena occurs in the steady-state condensation/vaporization of mixed vapors/liquids in wetted-wall towers. Unfortunately, several prominent transport texts assume that the ratio of molar fluxes is the same as the corresponding ratio of mole fractions at the interface for the phase being formed. This is shown to be true only at particular vertical positions corresponding to the first drop of condensate. The thermodynamics of the condensation/vaporization of mixtures is reviewed to understand why the ratio of pure-component fluxes at the interface differs from that of corresponding equilibrium mole fractions. The dynamics of steady-state condensation in wetted-wall towers is also developed based on the film theory of Colburn and Drew. The temperature/composition diagram is used to trace both transport phenomena and thermodynamic variables at various tower heights. The Ackermann factor is corrected allowing more general use of the design equations when the vapor is nonideal. The usual neglect of liquid-film resistance to heat transfer is examined. Numerical calculations show an unusual rise in the interfacial temperature in a parallel flow tower immediately below the onset of condensation. Possible and impossible sets of temperature and composition profiles are described.*

## Introduction

The condensation of mixed vapors, which is often encountered in industrial processes, requires an understanding of (1) the thermodynamics of fluid mixtures, (2) phase equilibria, (3) heat transfer, and (4) mass transfer. While the subject has a rich literature dating back to the 1930s for mixtures, its complexity is obvious from the many methods and assumptions used to design condensation towers. With modern computers, such assumptions can be tested and removed where necessary. We seek here to both provide new methods and a better understanding of the basics; that is why the following section looks at only the first two topics. The third section reviews the dynamic case involving also transport phenomena. Numerous errors in this literature have resulted from an incomplete understanding of the underlying thermodynamics. A simple example is that the composition of the condensate formed at the interface is, in general, neither that of the equilibrium vapor or liquid.

Only binary systems will be considered here, although the results can easily be extended to multicomponents. As applied to commercial, wetted-wall towers, the condensation will be considered isobaric and at steady state. Evaporation is just the reverse of condensation, and so the same principles apply, although resistances to heat and mass transfer may differ considerably.

Correspondence concerning this article should be addressed to P. T. Eubank.

## Thermodynamics and Phase Equilibria

### *Material balances*

Consider the complete thermodynamic equilibria case where the vapor and liquid phases are homogeneous with no thermal or compositional gradients. For a binary mixture in vapor–liquid equilibrium (VLE) at some pressure and temperature ($P$, $T$), all intensive variables are fixed under the Gibbs phase rule. When the overall composition $z(\equiv z_1)$ is also fixed, the lever rule (material balance) provides the relative amount of the two phases as $(V/L)=[(z-x)/(y-z)]=[q/(1-q)]$, where $q$ is the quality or fraction vapor (mole basis), $x$ is the liquid composition, and $y$ the vapor composition. Condensation and vaporization are reverse processes that may be performed at constant pressure $P$, as in heat

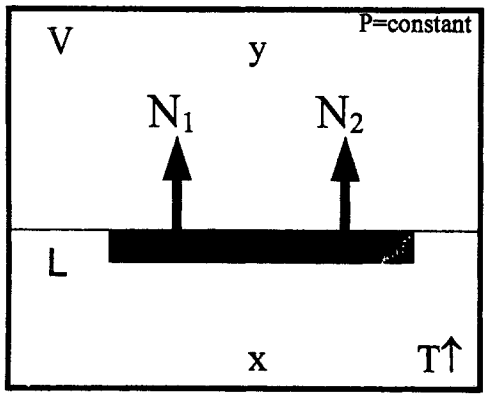


**Figure 1. Boiling at constant pressure for a binary system under complete thermodynamic equilibrium.**

exchangers, or at constant temperature $T$, as in some total-pressure measurement systems for VLE. Figures 1 and 2 show (1) a pictorial representation of boiling at constant $P$, and (2) the accompanying $T/x$ diagram, respectively:

If the still in Figure 1 was originally filled with liquid of overall composition $z$, then Figure 2 shows that the first bubble (bubble-point curve (BP)) of vapor would have a composition $y_B$ at the bubble-point temperature $T_B$, where $x = z$ and $q = 0$. As the vaporization proceeds, the temperature in the equilibrium still must increase. Figure 2 provides the liquid composition $x$ and the vapor composition $y$ for each $T$. The lever rule provides $q$ as long as we are inside the two-phase ($2\phi$) region. Finally, the dew-point (DP) temperature $T_D$ is reached with $x_D$ the composition of the last drop of liquid ($y = z$) or $q = 1$. Of course, the process can be reversed as condensation from the DP to the BP. The preceding discussion excludes the high-pressure phenomena of *retrograde condensation* where with increasing temperature at constant pressure a vapor mixture may first condense (retrograde), after which that condensate evaporates normally.

A common misconception is to view the crosshatched element of liquid in Figure 1 to be evaporated intact when indeed $x$, $y$, and $T$ are changing with this differential vaporization. The ratio of the amounts of components 1 and 2 differentially evaporated, the flux ratio $(N_2/N_1)$, is not generally $(1-x)/x$ nor $(1-y)/y$, as is often assumed in texts on transport phenomena (Bird et al., 1960; Slattery, 1972) and in the important work of Sparrow and Marschall (1969). The first authors are careful not to make this assumption in their text, but do so in Problem 18.N$_3$, where Eq. 18.N-1 is only correct for the initial condensate at the top of figure 18.N. The flux ratio $(N_2/N_1)$ is only the same as $(1-x)/x$ at a DP, whereas it is $(1-y)/y$ only at a BP. Transport phenomena texts often assume that it is the composition ratio of the *phase being formed*, but this violates thermodynamic reversibility and, thus, the second law of thermodynamics. We now derive a general thermodynamic relation for $(N_2/N_1)$ for the case of complete equilibrium (CTE).

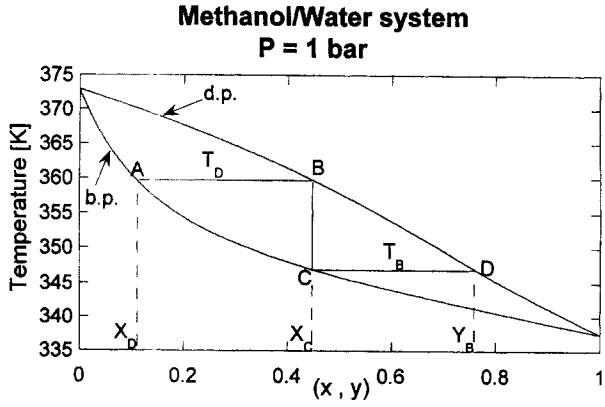


**Figure 2. Temperature/composition at constant pressure for a binary system, which is both volatile and condensable.**

In the differential vaporization (or condensation) process of Figures 1 and 2, the moles of evaporated component 1 are $d(Vy) = -d(Lx)$ and $d[V(1-y)] = -d[L(1-x)]$ for component 2. Thus, $(N_2/N_1) = [dq - d(qy)]/d(qy)$, where the quality $q \equiv V$. Since $[d(qy)/dq] = y + q(dy/dq)$,

$$(N_2/N_1) = \{[1 - y - q(dy/dq)]/[y + q(dy/dq)]\}. \quad (1)$$

From the lever balance rule, $q = [(z-x)/(y-x)]$ so $(-dq) = [(1-q)(dx) + q(dy)]/(y-x)$. Substituting the latter expression for $(dq)$ into Eq. 1 yields the major result for condensation/vaporization under complete equilibrium:

$$(N_2/N_1) = \{[(1-y)(1-q) + q(1-x)(\partial y/\partial x)_P]/[y(1-q) + qx(\partial y/\partial x)_P]\}. \quad (2)$$

Equation 2 is correct at the BP or at the DP or for any value of $q$. When the condensation/vaporization is at constant $T$, then a very similar equation results:

$$(N_2/N_1) = \{[(1-y)(1-q) + q(1-x)(\partial y/\partial x)_T]/[y(1-q) + qx(\partial y/\partial x)_T]\}. \quad (3)$$

Both $(\partial y/\partial x)_P$ and $(\partial y/\partial x)_T$ must always be positive as a condition of material stability; they are nonzero at azeotropes where $y = x$, as shown in Figure 3. At high dilution, $(\partial y/\partial x) \to K_1^\infty$ as $x \to 0$ and $(\partial y/\partial x) \to K_2^\infty$ as $x \to 1$. Evaluation of the limiting equilibrium constant $K_i^\infty$ in terms of Henry's constants and infinite dilution activity coefficients is given by Eubank et al. (1987).

These derivatives can be estimated from any VLE model, equation of state (EoS), or the gamma-phi ($\gamma$-$\phi$) method. A particularly simple case, which utilizes the premises of Raoult's law (no azeotropes possible), is where $P = (P_1^\sigma - P_2^\sigma)x + P_2^\sigma$ and $Py = P_1^\sigma x$. Then at constant $P$, $(\partial y/\partial x)_P \equiv [(\partial T/\partial x)_P/(\partial T/\partial y)_P] = \{[(y/r)P_1' + (1-y)rP_2']/[xP_1' + (1-x)P_2']\} \equiv (P_y'/P_x')$, where $r \equiv (P_1^\sigma/P_2^\sigma)$ and $P_i' \equiv (dP_i^\sigma/dT)$. The final result for Raoult's law is

$$(N_2/N_1) = \{[(1-y)(1-q)P_x' + q(1-x)P_y']/[y(1-q)P_x' + qxP_y']\}, \quad (4)$$

where $P'_y$ is also $[x(P_2^\sigma/P)P'_1 + (1-x)(P_1^\sigma/P)P'_2]$ under Raoult's law. For $(\partial y/\partial x)_T$, a similar procedure provides the simpler result,

$$(N_2/N_1) = \{[(1-y)(1-q)P^2 + q(1-x)P_1^\sigma P_2^\sigma] / [y(1-q)P^2 + qxP_1^\sigma P_2^\sigma]\}, \quad (5)$$

as $(\partial y/\partial x)_T = (P_1^\sigma P_2^\sigma/P^2)$ under Raoult's law. For hydrocarbon mixtures that condense at low to moderate pressures, this is a valid assumption. An EoS model must be used for high pressures, particularly where supercritical components are involved. For components that do not not form ideal liquid solutions, the $\gamma$-$\phi$ method may be used at low to moderate pressures, but the EoS must again be used at high pressures (e.g., with Wong-Sandler mixing rules and the Peng-Robinson EoS).

Numerical examples can be solved using (1) Raoult's law, (2) azeotropic systems, and (3) systems near the VL critical loci. Equations can also be developed for VLLE, where liquid-phase splitting can occur upon condensation.

### *Energy balances and heats of vaporization*

At any place in the two-phase region of Figure 2, the energy required to evaporate a differential amount of liquid of Figure 1 is termed the *differential heat of vaporization* $l_P$, where

$$l_p = T(\partial S/\partial q)_P, \quad (6)$$

where $S$ is the molar entropy. The *integral heat of vaporization*, $L_P$, on the other hand, is

$$L_P = \left[\int_0^1 l_P\,(dq)\right]_{P,[z_i]}, \quad (7)$$

which is the energy required to completely evaporate a mole unit of mixture at constant pressure, starting from its BP at the overall composition $z$ of Figure 2 and ending at the DP. An excellent discussion of differential and integral heats of vaporization can be found in the text of Bett et al. (1975). Here, we are primarily interested in the differential heat of vaporization, which Strickland-Constable (1951) found to be

$$l_P = \left\{\frac{(1-q)T(\partial x/\partial T)_P(\partial P/\partial T)_x[y\Delta\bar{v}_1 + (1-y)\Delta\bar{v}_2] + qT(\partial y/\partial T)_P(\partial P/\partial T)_y[x\Delta\bar{v}_1 + (1-x)\Delta\bar{v}_2]}{(1-q)(\partial x/\partial T)_P + q(\partial y/\partial T)_P}\right\} + \left\{\frac{(x-y)[(1-q)C_P^l + qC_P^v]}{(1-q)(\partial x/\partial T)_P + q(\partial y/\partial T)_P}\right\}, \quad (8)$$

where $\Delta\bar{v}_i \equiv \bar{v}_i^v - \bar{v}_i^l$ are the difference of partial molar volumes of species $i$ in vaporization; $C_P$ is the specific heat capacity; $(\partial P/\partial T)_x$ is the slope of the liquid isopleth or BP curve on a P/T diagram; and the superscripts $v$ and $l$ represent the vapor and liquid phases, respectively. The complicated Eq. 8 is a thermodynamic identity, whose first term is called *direct* and second *indirect*. The former is the change of entropy caused directly by evaporation of a drop of composition $Z$, while the latter is the change of entropy of each phase caused by the necessary change of temperature $(dT)$ accompanying the isobaric evaporation.

In terms of enthalpies, Eq. 8 is

$$l_P = [Z(\Delta\bar{H}_1) + (1-Z)(\Delta\bar{H}_2)] + \left\{\frac{(x-y)[(1-q)C_P^l + qC_P^v]}{(1-q)(\partial x/\partial T)_P + q(\partial y/\partial T)_P}\right\}, \quad (9)$$

where $Z$ is the actual composition of the drop of liquid evaporated or $[N_1/(N_1+N_2)] = [1+(N_2/N_1)]^{-1}$. The latter ratio follows from Eq. 2 as

$$Z = \left[\frac{(1-q)(\partial x/\partial T)_P y + q(\partial y/\partial T)_P x}{(1-q)(\partial x/\partial T)_P + q(\partial y/\partial T)_P}\right]. \quad (10)$$

Composition $Z$ changes from $y_B$ on the DP curve of Figure 2 $(q=0)$ to $x_D$, the last drop of liquid to evaporate $(q=1)$. Equation 10 shows $Z$ to be a weighted average of $x$ and $y$, and so, for cases of complete thermodynamic equilibria, it must always lie between the two; further, $Z$ should not be confused with the overall composition $z$. The indirect term of Eq. 9 appears to have always been rightfully neglected in the

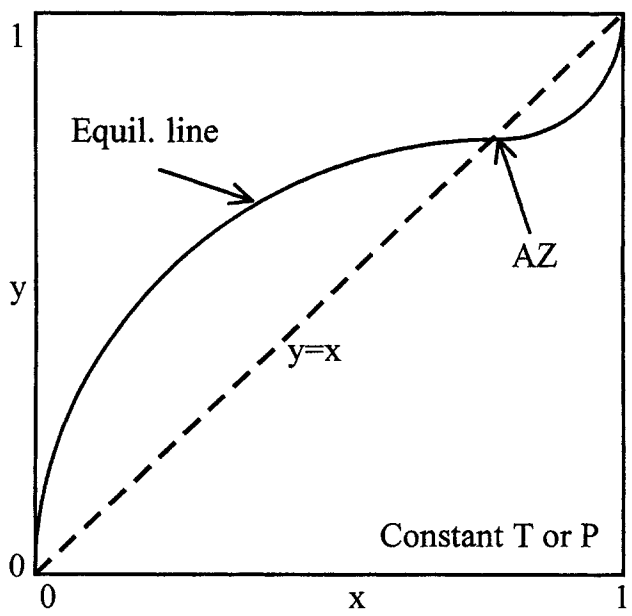


**Figure 3. A binary azeotrope at a given temperature or pressure.**

design of wetted-wall towers (Taylor and Krishna, 1993), a topic discussed in a later section. It is zero at azeotropic and pure end points, but does not vanish, in general, at either bubble or dew points. At the initial bubble point ($q = 0$), it reduces to $(\partial T/\partial x)_P(z - y_B)C_P^l$, whereas at the dew point ($q = 1$), it is $(\partial T/\partial y)_P(x_D - z)C_P^v$. Because liquid heat capacities are generally several times those of the corresponding vapor, this term usually contributes more to Eq. 9 near the bubble point, as shown by Bett et al. (1975) in an example with an equimolar mixture of oxygen (1) and nitrogen (2) at 1 bar where the indirect term contribution was 2.9% at the BP and 1.6% at the DP.

### *Rayleigh's equation*

A simpler case of local thermodynamic equilibrium (LTE) exists in differential distillation when the equilibrium vapor is continuously removed from the still, condensed, and collected as a homogeneous liquid not in equilibrium with the liquid remaining in the still. Instead of $d(Vy) = -d(Lx)$, we now have $y(dV) = -d(Lx)$ for differential evaporation and $d(Vy) = -xd(L)$ for differential condensation. Again with $-(dV) = (dL)$, the well-known Rayleigh equations result in

$$\ln(L/L_o) = \int_x^{x} \left(\frac{dx}{y-x}\right); \qquad \ln(V/V_o) = \int_z^{y} \left(\frac{dy}{x-y}\right), \quad (11)$$

where $L_o$ is the initial moles of liquid in the still for differential evaporation, and $V_o$ is the initial moles of vapor for differential condensation. Treybal (1980, p. 308) has integrated Eq. 11 under the assumption of constant relative volatility, $\alpha_{12} \equiv [y(1-x)/(1-y)x]$, under constant pressure. According to the premises leading to Raoult's law, $\alpha_{12} = [P_1^\sigma/P_2]$. Rayleigh-type equations also apply to a flowing vapor undergoing condensation as long as $x$ in the second equation just given is replaced by $Z$, the composition of the liquid formed at the interface (Colburn and Drew, 1937).

## Review of Heat- and Mass-Transfer Literature

### *Literature review*

Design methods to model falling film condensation can be separated into (1) two-dimensional models, (2) one-dimensional models, and (3) the equilibrium model.

1. Two-dimensional models are based on conservation laws and have been successfully used in modeling the condensation of a single component. They have had limited success in modeling multicomponent systems, however, because the solution is computationally intensive. Sparrow and Marschall (1969) used conservation laws for each phase to calculate heat-transfer resistances in the liquid and vapor phases, and composition profiles in the vapor phases. Their calculations assumed constant interfacial temperature and negligible mass-transfer resistance in the liquid phase. Denny and Jusionis (1972) used variable interfacial temperature with constant cooling water temperature to investigate the effect of forced flow on the heat-transfer resistances close to the entrance of the condenser. They reported a significant nonmonotonic change in the interfacial temperature and interfacial compositions. These authors assumed the bulk vapor composition to be constant, in essence assuming that the vapor phase was infinitely bounded. From a practical standpoint, the problem with two-dimensional models is that the complication of the second dimension does not give significantly better results in comparison to simpler one-dimensional models.

2. One-dimensional models, which form the basis for the section titled "Results from Design Calculations," are reviewed in detail later in this section. More recent works include Krishna and Standard (1976), who derived an exact matrix solution to Maxwell-Stefan equations by converting a two-component scalar problem into a multicomponent matrix problem. Earlier, Torr (1957) and Stewart and Prober (1964) proposed an approximate linearized theory for multicomponent diffusion based on the assumption that the effective diffusion coefficient remains constant through the film. Krupiczka et al. (1990) experimentally determined process parameters for countercurrent columns. They reported that their one-dimensional model fits the experimental data well and was within 30% for 85% of the points analyzed. Their analysis is based on assuming zero and infinite mass-transfer resistance in the liquid phase and then comparing these results to experimental data. Bandrowski and Kubaczka (1981) and Taylor and Smith (1982) studied the effect of thermal and diffusion resistances in a cocurrent column.

3. An equilibrium model, proposed by Silver (1947), modified by Bell and Ghaly (1972), and commonly referred to as the Silver–Bell method, is widely used by practicing engineers for the design of mixed-vapor condensers. Here, detailed mass-transfer equations are not used, and it is assumed that the gas remains saturated. Gas-side resistance is included by assuming the sensible heat change of the saturated gas mixture to be conducted through the gas film. The only data required are the dew-point and the bubble-point curves. The Silver–Bell method is preferred because little physical property data are needed. However, McNaught (1979) and Webb et al. (1996) have shown that large errors can result from using the Silver–Bell method relative to the one-dimensional film models of the previous paragraph. Further, Webb et al. (1996) have shown that the Silver–Bell method is very sensitive to the Lewis number ($Le = Sc/Pr$) for the vapor phase, and the calculated profiles should be used only when the Lewis number is close to or slightly less than unity. Also, they derived a correction factor that significantly reduces this error. This model remains viable because industrial design is very conservative.

In all of the preceding models, the mass transfer in the liquid phase is neglected by assuming that the flux mass-transfer coefficient, $\boldsymbol{k}^L$, is either infinity or zero. For an infinitely mixed condition, ($\boldsymbol{k}^L = \infty$), the interfacial liquid-phase composition equals the bulk condensate composition, and for an infinitely nonmixed condition, ($\boldsymbol{k}^L = 0$), the interfacial liquid-phase composition equals the flux composition $Z$. Kent and Pigford (1956) experimentally determined the liquid-phase flux mass-transfer coefficients, and these values are of the same order of magnitude as the vapor-phase flux mass-transfer coefficients. This implies that the flux mass-transfer resistance in both the liquid and vapor phases is important to the condensation process. Liquid-phase mass-transfer correlations are not available for falling film condensers, so the only recourse is to use the correlation derived for falling film evaporators. Recently, Palen et al. (1994) used the approxi-

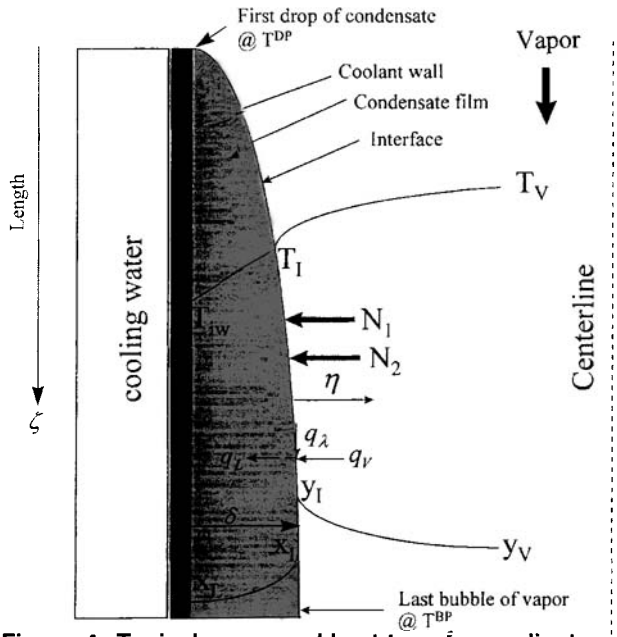


**Figure 4. Typical mass- and heat-transfer gradients and thermodynamics in a cocurrent condenser.**

This figure establishes the reference frame and the signs for rate terms in the text.

mate film-theory formulation to obtain a correlation for the liquid-phase mass transfer for a mixed-vapor evaporation from a falling film. The mass-transfer values calculated, by a hand calculator, from the Palen et al. (1994) correlation are in the same order of magnitude as the experimental values reported by Kent and Pigford (1956).

The recent text of Taylor and Krishna (1993) provides an excellent review of the entire field. We emphasize below points from the literature, providing thermodynamic insights, which later lead to our contributions.

### *Nusselt liquid-film condensation*

Equations for calculating the laminar liquid-film thickness $\delta_L$ with the vertical position $\zeta$ of Figure 4, and for the local heat-transfer coefficient, $h^L(\zeta)=(R_{Liq})^{-1}$ of Figure 5, for filmwise condensation of *pure* vapors were first obtained by Nusselt (1916) (see any heat-transfer text; e.g., Kreith, 1973):

$$\delta_L = \left[\frac{4\mu_L k_L \zeta (T_I - T_{iw})}{g\rho_L(\rho_L - \rho_V)\lambda}\right]^{1/4};$$

$$h^L = \left[\frac{g\rho_L(\rho_L - \rho_V)\lambda k_L^3}{4\mu_L \zeta (T_I - T_{iw})}\right]^{1/4}, \qquad (12)$$

where $h^L=(k_L/\delta_L)$, $k_L$ is the thermal conductivity of the liquid, $\mu_L$ its viscosity, and $\rho_L$ its mass density. $T_I$ is the interfacial temperature, whereas $T_{iw}$ is the inner wall temperature. Here we neglect changes in the area normal to the heat fluxes $q$ and to the mass fluxes $N_i$. Nusselt assumed that both the wall temperature and the interfacial temperature are constant; sensible heat term is taken into account for the vapor, and the temperature profile across the liquid film is assumed to be linear. Later, Sparrow and Marschall (1969) extended Nusselt's film theory to binary mixtures; here we use that treatment (Eq. 12) to provide local heat-transfer coefficients $h_\zeta^L$ only, whereas our vapor-side heat-transfer coefficients and both liquid- and vapor-side mass-transfer coefficients come from the very different film theory of Colburn and Drew (1937) below.

### *Two-film theory of Colburn and Drew*

In dynamic cases, such as the vertical tube condenser with a liquid film on the inner wall, LTE is assumed only at the gas/liquid interface, with neither the gas nor liquid phase homogeneous for some vertical position $\zeta$ at steady-state conditions. In classic two-film theory, there are resistances to both heat and mass transfer on both the gas and liquid sides of the interface, as shown by Figures 5 and 6, respectively. In Figure 5, $\boldsymbol{R}$ denotes a resistance to heat transfer according to Newton's law of cooling, and is the same as the reciprocal of the corresponding heat transfer coefficient $\boldsymbol{h}$, except that $\boldsymbol{R}_w$ is the wall thermal conductivity divided by the wall thickness. The heat flux $q_V$ is generally small compared to the heat of condensation $q_\lambda$ at the interface $I$. The resistance $\boldsymbol{R}_V$ increases ($\boldsymbol{h}^V$ decreases) as $\zeta$ increases for a downward-flowing gas, losing mass to condensation (Kent and Pigford, 1956). Obviously, the resistance $\boldsymbol{R}_L$ increases ($\boldsymbol{h}^L$ decreases as in Eq. 12) as $\zeta$ increases. In Figure 6, $\boldsymbol{M}$ represents the corresponding resistances to total mass transfer based on mole-fraction driving forces, so $\boldsymbol{M}$ is just the reciprocal of the mass-transfer coefficient thus defined. For Figures 5 and 6,

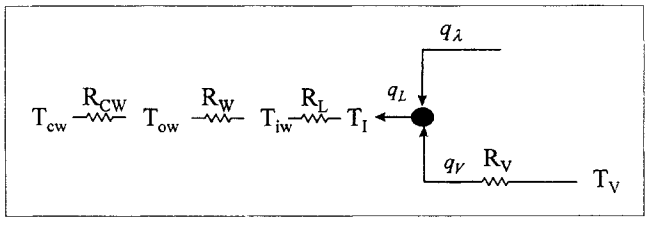


**Figure 5. Heat-transfer resistance for the condensation process.**

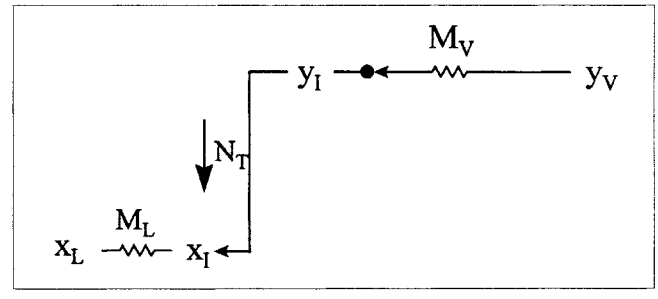


**Figure 6. Mass-transfer resistance for the condensation process.**

the static equilibrium case of the previous section (Figure 1) corresponds to zero values for all the resistances. We also acknowledge that the chemical potential of species $i$ is the correct potential function for diffusion as opposed to the corresponding mole fraction, but $\boldsymbol{M}$ also includes convection effects, so we will use the usual methods of mass transfer.

In the dynamic case, each resistance is influenced by molecular (conduction or diffusion) and bulk transport terms. This one-dimensional model was largely formulated in the 1930s by Othmer (1929), Colburn and Hougen (1934), and Colburn and Drew (1937), although film theory appears to have originated with Lewis and coworkers (Lewis, 1916; Lewis and Whitman, 1924; Lewis and Chang, 1928). Material balances take into account the change in mass and energy in each of the phases throughout the condenser. The accuracy of the model predictions is strongly dependent upon the accuracy of the correlations for the heat- and mass-transfer coefficients. Colburn and Drew (1937), in an extraordinary article exhibiting a superb grasp of both thermodynamics and transport phenomena, explained commercial data where one component was vaporized at the same time the second component was being condensed or $(N_2/N_1) < 0$, which leads to $Z$ being outside the interval (0,1), which is not possible at complete thermodynamic equilibria. Indeed, they first defined $Z$ and showed that it is neither the interfacial liquid composition $x_I$ nor the interfacial vapor composition $y_I$. For mass transfer across the gas film in Figure 4, they showed the molar flux of the first component to be

$$N_1 = wZ = -\boldsymbol{k}_y(dy/d\eta^*) + wy, \tag{13}$$

where the total condensation rate, $w = N_1 + N_2$; $\boldsymbol{k}_y$ is the mass transfer coefficient for the gas phase (Colburn and Drew used the symbol $F$); and $\eta^* \equiv (\eta/\delta_V)$ is the dimensionless distance across the gas film measured from the interface. Colburn and Drew omitted the negative sign in Eq. 13 and then used $w > 0$ to indicate condensation, despite having measured $\eta$ as shown in Figure 4. While this compensation works, we will save $w < 0$ for condensation and $w > 0$ for evaporation in keeping with our reference frame of Figure 4. If the mechanism for mass transfer in the gas film were purely diffusional, then $\boldsymbol{k}_y = (P\mathfrak{D}_{12}/RT\delta_V)$, where $\mathfrak{D}_{12}$ is the diffusion coefficient in the gas phase and $\delta_V$ is the thickness of the gas film. Equation 13 can be integrated between the limits of $\eta^* = 0$, $y = y_I$ and $\eta^* = 1$, $y = y_V$, the bulk value for the vapor, which varies only in the axial direction $\zeta$,

$$w = -\boldsymbol{k}_y \ln[(Z - y_I)/(Z - y_V)]. \tag{14}$$

The mole-fraction profile across the gas film is

$$y = Z - (Z - y_I)\exp[(w/\boldsymbol{k}_y)\eta^*]. \tag{15}$$

The diffusional contribution of Eq. 13 is then

$$J_1 = -\boldsymbol{k}_y(dy/d\eta^*) = \boldsymbol{k}_y(Z - y_I)\Phi\exp(\Phi\eta^*) = w(Z - y), \tag{16}$$

where $\Phi \equiv (w/\boldsymbol{k}_y)$, as used by Taylor and Krishna (1993, p. 154), in a development analogous to both Colburn and Drew and Bird et al. (1960). Replacing $Z$ in Eq. 16 yields, after some algebra,

$$J_1(\eta^* = 0) \equiv J_{1I} = \boldsymbol{k}_y\Phi(y_I - y_V)/[\exp(\Phi) - 1]$$
$$= \boldsymbol{k}_y\Xi_I(y_I - y_V) = \boldsymbol{k}^*_{yI}(y_I - y_V) \tag{17a}$$

$$J_1(\eta^* = 1) \equiv J_{1v} = \boldsymbol{k}_y\Phi[\exp(\Phi)](y_I - y_V)/[\exp(\Phi) - 1]$$
$$= \boldsymbol{k}_y\Xi_v(y_I - y_V) = \boldsymbol{k}^*_{yv}(y_I - y_V), \tag{17b}$$

which are the same as the Ackermann-type factors $\Xi$ of Taylor and Krishna (1993), allowing for a reversal of coordinates, and the same at the interface as that given by Bird et al. (1960, p. 663), who introduced the $\boldsymbol{k}^*$ symbol for coefficients at high rates of mass transfer. It is important to understand that the equations of Colburn and Drew (1937) include these corrections, and are not limited to low rates or to equimolar counterdiffusion, as has been suggested (Pratt and Tuohey, 1979).

The condensation rate and the heat flux at the interface, due only to condensation $q_\lambda$, are related by

$$q_\lambda = w\lambda_Z, \tag{18}$$

where $\lambda_Z$ is the direct term in the differential heat of condensation of Eq. 9, or

$$\lambda_Z = [Z(\Delta\overline{H}_1) + (1 - Z)(\Delta\overline{H}_2)]. \tag{19}$$

Colburn and Drew developed an energy balance that includes (1) the heat flux at the interface due only to condensation $q_\lambda$, (2) sensible heat loss by the gas film, and (3) sensible heat loss by the liquid film. They then both used an example and experience to show that the latter two effects are usually negligible in comparison to the first term. Then at any position $\zeta$

$$-w = [U(T_I = T_{cw})/\lambda_Z] = \boldsymbol{k}_y \ln[(Z - y_I)/(Z - y_V)]$$
$$= \boldsymbol{k}_x \ln[(Z - x_L)/(Z - x_I)], \tag{20}$$

where $x_L$ is the bulk liquid mole fraction of 1 and $\boldsymbol{k}_x$ is the liquid film mass-transfer coefficient.

The cooling water temperature $T_{cw}$ is known, as is $y_V$ and the overall heat-transfer coefficient $\boldsymbol{U}$, which is the reciprocal of the sum of the resistances $R_{cw}$, $R_w$, and $R_L$ of Figure 5, can be estimated. Resistance $R_L$ must be taken independently from a liquid film theory for heat transfer, such as Nusselt's theory, because the nature of the boundary conditions and temperature (or mole fraction) profiles are different for heat transfer across the liquid film than they are for heat transfer in the gas or mass transfer in either the gas or liquid. The three latter cases have a zero flux condition as we move away from the interface to either (1) the center line of Figure 4 for the gas, or (2) the inner wall/liquid boundary for the liquid.

The mass-transfer coefficient $k_y$ can be found from a $j$-factor correlation using data for the corresponding vapor-phase heat-transfer coefficient; $k_x$ can be found the same way in theory, but is more difficult to estimate accurately in practice. Since the pressure is fixed, the gas on the $T-x$ diagram of Figure 2 is cooled to the DP temperature—here $T_I$, where $Z = x_1$—near the top of the tower. As this also fixes the equilibrium mole fractions at the interface, Eq. 20 provides both $w$ and $Z$ without using the last equality, which is meaningless without a liquid film. Some trial and error is involved, as $\lambda_Z(Z)$.

In the general case of $\zeta \neq 0$, Eq. 20 remains valid, but the path followed on the $T-x$ diagram of Figure 2 is not vertical across the gas film. Colburn and Drew rewrote Eq. 20 as

$$Z = [y_V - y_1 E_V]/[1 - E_V], \tag{21}$$

where

$$E_V = \exp[-U(T_I - T_{cw})/\lambda_Z k_y] = \exp[w/k_y] = [(Z - y_V)/(Z - y_I)]. \tag{22}$$

Similar equations can be drawn on the liquid side with $Z = [x_I - x_L E_L]/[1 - E_L]$, where $E_L = \exp[-U(T_I - T_{cw})/\lambda_Z k_x] = \exp[w/k_x] = [(Z - x_I)/(Z - x_L)]$. Then, as discussed by Colburn and Drew, $E_V$ and $E_L$ can only lie between zero and unity for condensation. As commonly occurs for condensation, $y_V < y_I$ for the light-behaving component ($x_I < y_I$), then $Z$ is negative for low $(-w)$ and positive for higher values as shown by Figure 7 ($y_V = 0.7$; $y_I = 0.8$). We found these relations easier to follow using a rearrangement of Eq. 22:

$$(y_V - Z) = [\exp(-w/k_y) - 1]^{-1}(y_I - y_V), \tag{23}$$

with Figure 8 showing that for $(-w/k_y) = 0.12$, a low condensation rate, the slope of the straight line, is $[\exp(-w/k_y) - 1]^{-1}$, or 7.84, causing the difference $(y_I - y_V)$ to be increased in terms of $(y_V - Z)$. Thus, when $y_V < y_I$, by say only 0.1, as for Figure 7, $(y_V - Z) = 0.78$, meaning if the vapor feed composition is less than this value we would have a negative value of $Z$, here $-0.084$. The case of $y_V > y_I$, cited by Colburn and Drew, is a stranger situation for condensation, as $(y_V - Z)$ will be negative, indicating that the light component is preferentially condensing and $Z$ may be driven higher than unity; this, however, should be expected when condensing a gas with $y_V > y_{AZ}$, for systems forming positive azeotropes (+AZ), or the reverse for systems forming negative azeotropes (−AZ).

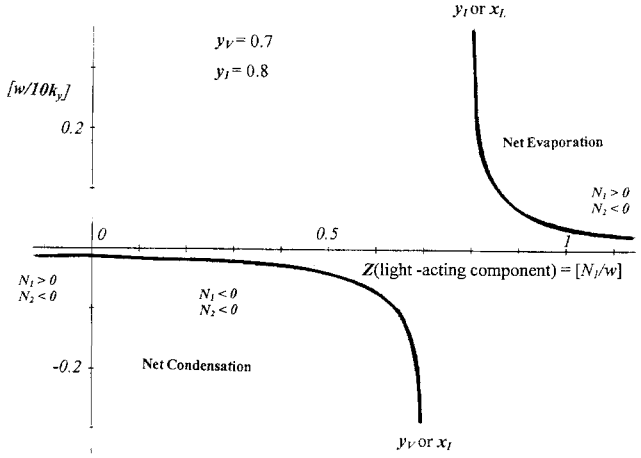


**Figure 7. Net evaporation or condensation as a function of $Z$ (the ratio of the molar flux of component 1, $N_1$ to the net flux, $[(N_1 + N_2)]$ for $y_I = 0.8$ and $y_v = 0.7$).**

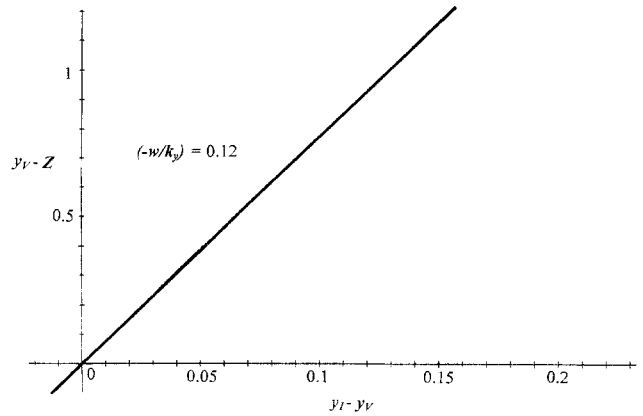


**Figure 8. Difference between bulk vapor composition and $Z$ vs. the difference between interfacial vapor and bulk vapor compositions for a low rate of condensation corresponding to $(w/k_y) = 0.12$; the relation is linear and so may be extrapolated.**

Van Es and Heertjes (1962) gave another view of $Z$ as the value of $y$ as $\eta \to \infty$ in their figure 4. That is, at the right edge of the gas film, $y$ is $y_v$, but $(dy/d\eta^*) = \Phi(y_V - Z) \neq 0$. A nonphysical extrapolation of this curve $y(\eta^*)$ to higher values of $\eta^*$ leads to $y = Z$ in Eq. 15 as $\eta \to \infty (w < 0)$. This approach shows that $y_V$ must lie between $y_I$ and $Z$ for net condensation, as with Eq. 14, whereas $y_I$ lies between $y_V$ and $Z$ for net evaporation, and $Z$ cannot lie between $y_I$ and $y_V$ for either case.

To solve for an incremental column height $\Delta\zeta$, the complete form of Eq. 20 is generally necessary. The unknowns are $Z$, $w$, and $T_I$, and Eq. 20 provides three equalities so a solution by trial and error is possible when $U$, $T_{cw}$, $\lambda_Z(Z)$, $k_y$, $k_x$, $h^V$, $y_V$, and $x_L$ are known. To proceed down the tower for the next increment column height $\Delta\zeta$,

$$VC_P^v(dT_V/dA) = -h^V(T_V - T_I)\{\Phi_H/[\exp((\Phi_H) - 1)]\} = -h^V(T_V - T_I)\Xi_H = -h^{\cdot V}(T_V - T_I), \tag{24}$$

where $V$ (moles/time) is the total vapor flow rate; $A$ is the area of the cooling surface; $\Phi_H \equiv (-wC_{PZ}^v/h^V)$, where molar heat capacity of the vapor is $C_P^v = y_v C_{P1}^v + (1 - y_v)C_{P2}^v$ evaluated at $T_V$, but $C_{PZ}^v = ZC_{P1}^v + (1 - Z)C_{P2}^v$ is evaluated at the mean of $T_V$ and $T_I$. The factor $\Xi_H$ is the original Acker-

mann correction for heat transfer (Ackermann, 1937), like the similar correction to mass-transfer coefficients, Eq. 17, both for high mass-transfer rates. Further,

$$(dT_V/dy_V) = [(T_V - T_I)/(Z - y_V)][C_{PZ}^v/C_P^v]/[\exp((\Phi_H) - 1)]. \quad (25)$$

When Eq. 25 is combined with Rayleigh's equation for the gas,

$$(dy_V/dA) = [-w(y_V - Z)/V]. \quad (26)$$

### *Partial condenser equations of Kent and Pigford*

Here Eqs. 15 (with $\eta^* = 1$) and 28 [with $w = (dV/dA)$] of Colburn and Drew are combined to show that the number of transfer units

$$\int_{y_{v_1}}^{y_{v_2}} \left( \frac{dy}{y_I - y_v} \right) = \int_{V_1}^{V_2} \left\{ \frac{d \ln V}{1 - \exp(-w/k_y)} \right\}, \quad (27)$$

where the subscripts 1 and 2 indicate vertical positions in the tower. Because the gas phase would be in turbulent flow, it is assumed that $k_y$ is proportional to $V$; furthermore, $w$ is replaced by $-[(V_1 - V_2)/\pi D\zeta]$, where $D$ is the tower diameter. Then using the log-mean average of $k_y$, it is shown that an average value of $(-w/k_y) = (V/k_y)_1(\pi D\zeta)^{-1} \ln(V_1/V_2)$, allowing for simple integration of Eq. 27 with the denominator taken as a constant. The correct result is

$$N_G = \left[ \frac{\ln(V_1/V_2)}{(V_1/V_2)^{([V/k_y)_1]/\pi D\zeta)} - 1} \right], \quad (28)$$

but unfortunately equation 14 of Kent and Pigford (1956) was printed with the denominator of Eq. 28 as $1 - (V_1/V_2)^{-([(V/k_y)_1]/\pi D\zeta)}$, which is different. A graph (Figure 1 of Kent and Pigford) of $N_G$ vs. $\ln(V_1/V_2)$ was provided for the incorrect equation, with $(k_y/V)_1(\pi D\zeta)$ as a parameter. The left side of the graph corresponds to a negligible rate of condensation, or $(V_1/V_2) \to 1$, which by L'Hopital's rule is just the value of the parameter $(k_y/V)_1(\pi D\zeta)$ for either version of Eq. 28. In our Eq. 28, however, $N_G$ will decrease with increasing $(V_1/V_2)$, whereas it increases in Figure 1 of Kent and Pigford. Rayleigh's equation (Eq. 11) for differential condensation corresponds to zero gas-side resistance to mass transfer, but infinite liquid-side resistance, as the liquid drops are removed when formed; that is, $k_y$ is infinite but $k_x$ is zero. These values are reversed on Figure 1 of Kent and Pigford, although Rayleigh's equation of $N_G = \ln(V_1/V_2)$ is correctly graphed. The authors are misled into stating that for large values of $(V_1/V_2)$, $N_G$ is independent of the gas-side resistance to mass transfer and can be calculated from Rayleigh's equation. It is then understood that Rayleigh's equation should not be graphed on Figure 1 of Kent and Pigford, which is captioned "Partial condensation in countercurrent column: gas-film resistance only," because here the liquid-film resistance is zero, whereas in Rayleigh's equation it is infinite. Whether flow is parallel or countercurrent makes no difference here, as the liquid-phase resistance is zero. Figure 9 is the corrected version of Figure 1 of Kent and Pigford; when the parameter $(k_y/V)_1(\pi D\zeta)$ is zero, then the denominator of Eq. 28 diverges, causing $N_G$ to be zero. $N_G$ is divergent when $(k_y/V)_1(\pi D\zeta)$ is infinite, corresponding to no resistance to mass transfer in either phase; this would also correspond to the earlier case of complete thermodynamic equilibrium if there also were no thermal gradients.

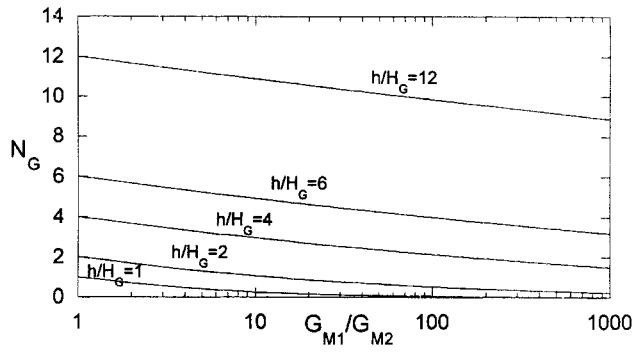


**Figure 9. Number of transfer units as a function of the logarithm of the ratio of inlet to existing gas flow rates.**

This figures corrects Figure 1 of Kent and Pigford (1956) so that it is consistent with other figures and equations in that publication.

This error in the work of Kent and Pigford is mystifying, because they go on to correctly derive a general equation (their Eq. 16; see their appendix) for the case of where the liquid-film resistance is not zero, using a corresponding parameter $(k_x/L)_1(\pi D\zeta)$. The corresponding Figure 2 of Kent and Pigford and the description of Rayleigh's equation following their equation 16 are likewise correct, as is their comparison to experimental data in their Figure 5. Indeed, the curve of $(k_x/L)_1(\pi D\zeta) = \infty$ on the bottom panel of their Figure 2, $(k_y/V)_1(\pi D\zeta) = 1$, must be the same as the corresponding curve on their Figure 1, but it is not. Replacement of their Figure 1 by our Figure 9 restores consistency with their Figure 2 and, indeed, with the remainder of their work. Most of the equations of Kent and Pigford, including equation 16, apply to either countercurrent or parallel flow, although some intermediate equations require a change of sign, as $dV = -dL$ for parallel flow, whereas $dV = dL$ for countercurrent; further, these authors followed Colburn and Drew (1937) in assuming $w$ to be positive for condensation.

## New Developments in Theory and Understanding

### *Mole fraction profiles in wetted-wall towers*

Temperature profiles in wetted-wall towers are as in Figure 4 (see also Figure 5), with decreasing temperature as one moves from the center line to the cooling water at fixed elevation $\zeta$. The mole fraction or composition profiles can take several different possible forms, however, and a number of such diagrams appearing in mass-transfer texts are not possible. Here we assume that the liquid film is always flowing downwards due to gravity, whereas the gas can be flowing

either upwards (countercurrent to the liquid) or downwards (parallel to the liquid). In Figure 4, $y_I > x_I$, so we conclude that $y$ and $x$ represent the mole fraction of the more volatile component or, at least, the component behaving more volatile when the system is azeotropic. Moving from the center line of Figure 4 toward the interface there is an adverse gradient of $y$, meaning the more volatile component tends to diffuse toward the center line, whereas the heavier component diffuses toward the interface. Because the heavier component is preferentially condensed from the bulk vapor, $Z \equiv [N_1/(N_1 + N_2)] < y_V$ in agreement with the Van Es and Heertjes (1962) notion, discussed earlier, that $Z$ is the asymptotic value of the $y$ profile extrapolated to $\eta \to \infty$. Further, the liquid-film profile of Figure 4 shows a lower mole fraction of the light component in the bulk as opposed to the interface, because the bulk liquid is from condensate above (lower $\zeta$), which for parallel flow condensed at higher temperature, lower $y_I$ and $x_I$ (see Figure 2), and lower $Z$. Inversion of the mole fraction profiles of Figure 4 provides a possible diagram for the heavy component.

As shown previously by Eqs. 21 and 22 and Figures 7 and 8, the light-behaving component ($y_I > x_I$) must preferentially remain in the vapor with condensation ($Z < y_V$), whether flow is parallel or countercurrent. It has also been shown that the value of $Z$ cannot lie between $y_V$ and $y_I$, so for condensation $Z < y_V < y_I$, when it is understood that the first component is *behaving* as the more volatile component. For any such published mole fraction diagram involving both the gas and liquid phases at some elevation in the tower, it is obvious from the magnitudes of $y_I$ and $x_I$ whether the light or heavy component mole fraction is being graphed. The diagram may or may not specify whether it is for (1) condensation or vaporization, or (2) parallel or countercurrent flow. The more specified, the more carefully must the diagram be drawn, so as not to violate the preceding discussion. For condensation, there are only two choices: (1) Figure 4 when flow is parallel, and (2) Figure 4, but with the liquid profile inverted ($x$ increasing from the interface to bulk (right-to-left)) when flow is countercurrent.

For *condensation* the vapor is cooled as it flows through the tower, so by Figure 2 the interfacial temperature is expected to fall while $y_I$ and $x_I$ increase in the direction of gas flow (an anomalous exception occurring at the gas entrance is discussed below). Then $N_2 < 0$, $N_2 < N_1$, and $(dy/d\eta) < 0$, so for the heavy component 2, diffusion and bulk flow must both be in the negative $\eta$ direction toward the interface of Figure 4. However, $N_1$ can be either negative ($0 < Z < 0.5$) or positive ($Z < 0$). When $N_1 = 0$, the diffusional and bulk contributions are equal but opposite, corresponding to a noncondensible component and $y_V = y_I E_V$ from Eq. 21. For *vaporization* or net evaporation, the liquid is heated so the interfacial temperature is expected to rise in the direction of liquid flow as the more volatile-behaving component (here, 1) is preferentially removed. Then $N_1 > 0$ and $N_2 < N_1$ and $(dx/d\eta) < 0$, so for the light component 1 diffusion and bulk flow must both be in the positive $\eta$ direction toward the interface. However, $N_2$ can be either positive ($0.5 < Z < 1$) or negative ($Z > 1$). When $N_2 = 0$, the diffusional and bulk contributions are equal but opposite, corresponding to a nonevaporable component and $x_{2I} = x_{2L} E_L$ from the equation following Eq. 22. In summary, the heavy-behaving component must be diffusing in the gas phase toward the interface in net condensation, whereas the light-behaving component must be diffusing in the liquid phase toward the interface in net evaporation.

Two examples from the literature are now provided. First, Figure 5.2 of Treybal (1980) shows positive values for both $(dx/d\eta)$ and $(dy/d\eta)$ across the liquid and gas films, respectively, but $y_I < x_I$, so the figure is for the less volatile-behaving component. $Z$ ($N_1$ is now for the heavy component) $> y_V$, so condensation would occur; Treybal is safe in not specifying condensation or vaporization. The liquid profile shows $x_I > x_L$, however, so flow must be countercurrent, which is also not specified by Treybal. The second example is Figure 15.4 of Taylor and Krishna (1993), which has the caption: "Composition and temperature profiles in condensation." Again both $(dx/d\eta)$ and $(dy/d\eta)$ are positive, but $y_I > x_I$, so the vapor profile predicts that condensation is preferable to the volatile component (see Figure 7), whereas the liquid profile predicts that evaporation is preferable to the heavy component; thus, the diagram is not possible for either condensation or evaporation. The figure can be made consistent (1) for evaporation by inversion of the liquid profile so that $(dx/d\eta) < 0$, or (2) for condensation by (a) moving the entire liquid profile upwards so that $y_I < x_I$, to correspond to the first example from Treybal and to Figure 11.1 of Taylor and Krishna, or (b) inversion of the gas profile so that $(dy/d\eta)$ is negative, so the entire diagram corresponds to Figure 4.

We have picked on two of our favorite mass-transfer texts to illustrate that the drawing of mole fraction profiles across the gas and liquid films cannot be done without many implications concerning whether (1) condensation or vaporization is occurring, (2) the flow is parallel or countercurrent, or (3) any of these scenarios are possible.

### *Additional uses of the T/x diagram*

Figure 10 shows lines of constant axial position on a temperature/composition for a steady-state, parallel-flow con-

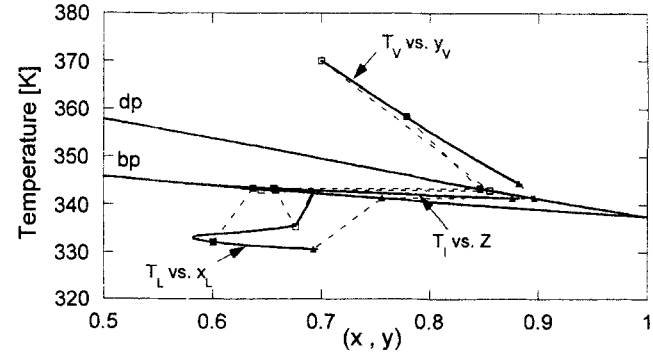


**Figure 10. Vapor-phase profile ($T_V$ vs. $y_V$), condensation rate profile ($T_I$ vs. $Z$), bulk-liquid phase profile ($T_I$ vs. $x_L$), dew-point curve ($DP$), and bubble-point curve ($BP$) are shown for a methanol/water system on a *Txy* diagram at one atmosphere.**

Composition and temperature are shown for selected isoposition lines: $\zeta = 0$ m (□) $\zeta = 2$ m (■), and $\zeta = 3$ m (▲).

denser operating at a fixed pressure (1 bar) with the methanol(1)/water(2) system. While such a diagram is considered *thermodynamic*, as it provides the phase equilibria at the vapor–liquid interface of Figure 4, it also shows the temperature and composition variations across the gas and liquid films, and so provides a rather complete picture of what is taking place in the condenser. The entering bulk vapor has roughly 30° of superheat, and the locus of the bulk vapor $(T_V, y_V)$ is shown in Figure 10 (and Eq. 24). The bulk vapor locus must approach the dew-point locus as the condensing gas descends through the tower. If all of the gas is condensed, the bulk vapor locus terminates at a dew point. Also shown in Figure 10 is the bulk liquid locus $(T_L, x_L)$, which must begin on the bubble-point curve, but then is expected to move to lower temperatures *and* higher values of $x_L$ as the liquid film is cooled and receives more of the light component via condensation. While Figure 10 does show that the temperature of the bulk liquid drops monotonically, the interfacial temperature shows a slight increase at the top of the tower before its normal descent down the tower (increasing $\zeta$); this causes $x_L$ to suffer an initial decrease before its normal increase. This interesting anomaly, which to our knowledge has not been reported either from experiment or calculations, is discussed in a later section. Also shown in Figure 10 is the locus of $Z$ vs. the interfacial temperature, $T_I$. Here $Z$ simply runs from a point on the bubble-point curve at the top of the tower to a higher value on the dew-point curve, corresponding to the composition of the last bubble of vapor. It should be recalled that $Z$ can assume negative values in some net condensation examples, for some $\zeta$.

For simplicity we have drawn straight lines across the vapor film from the bulk vapor $(T_V, y_V)$ to the interface $(T_I, y_I)$ for fixed $\zeta$, as well as across the liquid film. These lines are not likely to be straight, as $y$ is nonlinear with $\eta$ according to Eq. 15, whereas the local temperature is also nonlinear with $\eta$, as shown in the following section. Nevertheless, the slope of these straight lines is $[(T_V - T_I)/(y_V - y_I)]$ for the vapor film and $[(T_I - T_L)/(x_I - x_L]$ for the liquid film in reference to the driving forces for Figures 5 and 6.

### *Correcting the Ackermann correction for nonideal solutions*

The original Ackermann correction for heat transfer (Ackermann, 1937), $\Xi_H$ of Eq. 24, was derived based upon an ideal solution assumption for the gas phase. Here we provide a more general result for the Ackermann correction, removing the ideal solution assumption. This further correction should be especially important for gases at high pressures when polar components are present. Although we have no Ackermann correction for liquid-side heat transfer in our present condensation model using Nusselt's theory rather than the more general Colburn and Drew theory, we will use a two-film approach in this section for heat-transfer coefficients, following the development in chapter 11 of Taylor and Krishna (1993). Physically, there is no question that heat transfer and heat-transfer coefficients are enhanced due to mass fluxes in the liquid film in the $\eta$ direction; that is, Ackermann corrections for liquid-side heat transfer do exist but are usually not important, as the uncorrected heat transfer coefficient is already very high, as argued by Taylor and Krishna (1993).

In agreement with Figure 5, the total energy flux at the interface is

$$q_L = q_\lambda + q_V,$$

where

$$q_\lambda = \sum_{i=1}^{C} N_i\left(\overline{H}_i - \overline{h}_i\right), \qquad q_V = -k_V(dT/d\eta)_{\eta=0+},$$

$$\text{and} \qquad q_L = -k_L(dT/d\eta)_{\eta=0-}, \quad (29)$$

where $\overline{H}_i$ is the partial molar enthalpy of component $i$ in the vapor, $\overline{h}_i$ is the partial molar enthalpy of component $i$ in the liquid, and $k_V$ is the vapor thermal conductivity. The energy flux $\mathcal{E}$ is constant across the gas film when defined as

$$\mathcal{E}_{\mathcal{V}} = \sum_{i=1}^{C} N_i\overline{H}_i - k_V(dT/d\eta), \quad \text{for} \quad \eta \geq 0;$$

$$\mathcal{E}_{\mathcal{L}} = \sum_{i=1}^{C} N_i\overline{h}_i - k_L(dT/d\eta), \quad \text{for} \quad \eta \leq 0, \quad (30)$$

with $\mathcal{E}_{\mathcal{V}} = \mathcal{E}_{\mathcal{L}}$ at interface. For steady state, $(d\mathcal{E}/d\eta) = 0$ at any position in either the gas or liquid film; then (using gas-side notation):

$$w\sum_{i=1}^{C} Z_i(\partial\overline{H}_i/\partial\eta)|_P = k_V(d^2T/d\eta^2), \quad (31)$$

where

$$(\partial\overline{H}_i/\partial\eta)|_P = (\partial\overline{H}_i/\partial T)|_{P,y}(dT/d\eta)_P + (\partial\overline{H}_i/\partial y)|_{P,T}(dy/d\eta)_P. \quad (32)$$

From Eq. 16,

$$(dy/d\eta)_P = \{\Phi(y_v - y_I)\exp(\Phi\eta)/\delta_V[\exp(\Phi) - 1]\}, \quad (33)$$

whereas the two thermodynamics derivatives are

$$(\partial\overline{H}_i/\partial T)_{P,y} \equiv \overline{C}_{P,i};$$

$$(\partial\overline{H}_i/\partial y)_{P,T} = -RT^2\left.\frac{\partial}{\partial T}\right|_{P,y}\left(\frac{\partial \ln\gamma_i}{\partial y}\right)_{P,T}, \quad (34)$$

where $\overline{C}_{P,i}$ is the partial molar heat capacity and $\gamma_i$ is the activity coefficient, both of component $i$ in the mixture. Equations 31–34 can be combined and the second-order linear ODE integrated twice with previous boundary conditions to provide the temperature profile across the gas film as

$$\left[\frac{T-T_I}{T_v-T_I}\right]=\left[\frac{\Gamma(e^{\Phi\eta}-1)}{\Phi(\Phi-\Phi_H^*)}\right]+\left[\frac{\Phi(\Phi-\Phi_H^*)-\Gamma(e^{\Phi}-1)}{\Phi(\Phi-\Phi_H^*)(e^{\Phi_H^*\eta}-1)}\right](e^{\Phi_H^*\eta}-1), \quad (35)$$

where

$$\Gamma\equiv[w\delta_V\Phi(y_v-y_I)/k_V(T_v-T_I)(e^{\Phi}-1)]\sum_i Z_i(\partial\overline{H}_i/\partial y)_{P,T} \quad (36)$$

and

$$\Phi_H^*\equiv\left[w\delta_V\Phi\left(\sum_i Z_i\overline{C}_{P,i}\right)/k_V\right]. \quad (37)$$

At the interface,

$$q_V=\Xi_H^*h(T_I-T_v), \quad (38)$$

where

$$\Xi_H^*=\left[\frac{\Gamma\Phi(e^{\Phi_H^*}-1)+[\Phi(\Phi-\Phi_H^*)-\Gamma(e^{\Phi}-1)]\Phi_H^*}{\Phi(\Phi-\Phi_H^*)(e^{\Phi_H^*}-1)}\right], \quad (39)$$

so

$$\mathcal{E}_{\mathcal{V}}=\Xi_H^*h(T_I-T_v)+w\sum_i Z_i\left[C_{P,i}^*(T_I-T_{Ref,i})+H_i^{Res}-RT_I^2\frac{\partial}{\partial T}\bigg|_{P,y}\left(\frac{\partial\ln\gamma_i}{\partial y}\right)_{P,T}\bigg|_{T_I}\right], \quad (40)$$

where $C_{P,i}^*$ is the perfect (ideal) gas-state heat capacity of pure $i$, $T_{Ref,i}$ is the perfect gas-state reference temperature of pure $i$ (where $H_i^*$ has been set to zero) and $H_i^{\mathrm{Res}}$ is the residual enthalpy of pure $i$ at $(P, T_I)$—see Smith et al. (1996). Analogous equations can be derived on the liquid side for examples where the Colburn-Drew theory is being used, while liquid-side correction via Eq. 39 will yield $\Xi_{H,L}^*$ values that are very different from $\Xi_{H,L}$ for highly nonideal liquids such as methanol/water. As noted in the introduction to this section, the practical importance of this additional correction is not great, as the uncorrected heat-transfer coefficients are already very high ($R_{liq}$ low) in a system (Figure 5) where other resistances in series are higher.

Equality of $\mathcal{E}_{\mathcal{V}}$ with $\mathcal{E}_{\mathcal{L}}$ at the interface eliminates terms involving $C_{P,i}^*$, and with it the reference states

$$\Xi_{H,V}^*H_V(T_v-T_I)-\Xi_{H,L}^*h_L(T_I-T_l)=w\sum_i Z_i\left[(H_{i,V}^{\mathrm{Res}}-H_{i,L}^{\mathrm{Res}})-RT_I^2\left[\frac{\partial}{\partial T}\bigg|_{P,y}\left(\frac{\partial\ln\gamma_i}{\partial y}\right)_{P,T}\bigg|_{T_I}-\frac{\partial}{\partial T}\bigg|_{P,x}\left(\frac{\partial\ln\gamma_i}{\partial x}\right)_{P,T}\bigg|_{T_I}\right]\right]. \quad (41)$$

Gas-side activity coefficients are commonly replaced by a ratio of the mixture fugacity coefficient to the fugacity coefficient of the pure component at mixture pressure and temperature. When both the gas and liquid films are assumed to be ideal solutions, Eq. 41 reduces to

$$\Xi_{H,V}h_V(T_v-T_I)-\Xi_{H,L}h_L(T_I-T_l)=w\sum_i Z_i[(H_{i,V}^{\mathrm{Res}}-H_{i,L}^{\mathrm{Res}})], \quad (42)$$

where $\Xi_H$ is defined under Eq. 24. This simplification is due to $\overline{C}_{P,i}=C_{P,i}$ when the solution is ideal. When the gas phase is also a perfect (ideal) gas mixture, Eq. 42 is further simplified as $H_i^{\mathrm{Res}}=0$ for the vapor, and $\Xi_H$ for the vapor is evaluated with $C_{P,i}=C_{P,i}^*$; these are essentially the assumptions behind Raoult's law.

### *Azeotropic VLE*

We end this section with some comments about the condensation of an azeotropic vapor. Except for the possibility of the reversal of volatility, the presence of an azeotrope does not generally complicate condensation. As in other processes, the azeotrope acts like a pure component has been placed in the middle of the $T/x$ diagram. Condensing a mixture with the more common positive azeotrope (minimum boiling) will result in interfacial conditions that approach azeotropic proceeding in the direction of vapor flow, assuming that the vapor is cooled in its direction of flow. Condensation with a negative azeotrope would conversely lead the interfacial conditions away from the azeotrope. These conclusions normally would be reversed for evaporation.

When the inlet vapor is saturated (e.g., on the dew-point curve of a $T/x$ diagram), then that is the initial interfacial condition, and it will be on one side of the azeotrope or the other. While a vapor/liquid azeotrope may shift its composition, temperature, and pressure, it cannot shift if the pressure (or temperature) is held fixed, because azeotropic constraints cause the Gibbs phase rule to yield a univariant system, regardless of the number of components. When, as in Figure 10 (no azeotrope shown), the inlet vapor is not saturated, then an interesting situation arises where the change in $y$ across the gas film is $(y_I-y_V)$, which could bridge the azeotrope. However, Eq. 15 can be rearranged to

$$y_I-y_V=(y_I-Z)[1-\exp(w/\boldsymbol{k}_y)]. \quad (43)$$

For the first drop of condensate, $Z=x_I$, so since the bracketed term is always positive for condensation ($w<0$), the azeotrope cannot be bridged, as $y_V$ and $x_I$ must both lie on the same side of $y_I$ on the $T/x$ diagram. When $y_V$ corresponds to an azeotropic composition at the tower pressure, $y_I$ and $x_I$ will assume the same value, even though the vapor is superheated.

## Results from Design Calculations

First we show results from solving the energy and material balance equations, together with the assumed equilibrium at

the interface for small increments of elevation, $\Delta\zeta$, starting at the top of a parallel (cocurrent) flow tower for methanol(1)/water(2) at 1 bar, as depicted in Figures 2 and 4. The numerical procedure, which is similar to that in example 15.1.1 of Taylor and Krishna (1993), specifically uses Eqs. 20, 24, the liquid-side equivalent of Eq. 24, Eq. 41 accounting for nonideal liquid effects, and the usual dew and bubble criteria. (We agree with Taylor and Krishna that the average interfacial temperature for each sequential increment of elevation is the key variable to assume to initiate the numerical calculations because interfacial mole fractions are also then fixed.) Such initial guesses should always be made with possible two-phase temperatures lying between bubble- and dew-point curves on $T/x$ diagrams, such as Figure 10. Even with highly superheated bulk vapors ($T_V$, $y_V$) entering the section $\Delta\zeta$, all of our results show that the converged average interfacial temperature lies between the bubble and dew curve at $y_V$. While exceptions obviously exist, it is generally efficient to take the midpoint between the bubble and dew curve at $y_V$ as the initial guess of $T_I$ for each new section $\Delta\zeta$.

The numerical calculations performed make no assumptions about the liquid-phase mass-transfer coefficients, an important distinction, because the resulting composition profiles can be quite different. The two opposite assumptions commonly made about the liquid phase are:

1. The mass-transfer coefficient is infinitely nonmixed, $k_L = 0$, so the liquid-phase interface composition, $x_I$, equals the condensing composition, $Z$.
2. The mass-transfer coefficient is infinitely mixed, $k_L = \infty$, so the liquid-phase interface composition, $x_I$, equals the condensate composition, $x_L$.

The mass-transfer coefficient in the condensate is calculated using the Palen et al. (1994) correlation for the Sherwood number,

$$Sh^l \equiv \frac{k^l \delta^l}{D^l_{AB}} = 0.00631(Re^l)^{0.931}(Sc^l)^{0.5}. \tag{44}$$

The heat transfer in the condensate is calculated using the Nusselt solution (1916). The vapor-phase heat- and mass-transfer coefficients are estimated using the well-known Colburn and Chilton $j$ correlation (1937):

$$j = \frac{k^v MW^v}{G^v}\left(\frac{\mu^v}{\rho^v D^v_{AB}}\right)^{2/3} = \frac{h^v MW^v}{G^v}\left(\frac{C^v_p \mu^v}{k^v_T}\right)^{2/3}, \tag{45}$$

where $j$ is estimated using the Schrodt and Gerhard (1968) correlation:

$$j = 0.79(Re^v)^{-0.475}. \tag{46}$$

The heat-transfer coefficient in the coolant water, $h_{cw}$, is estimated using the correlation prescribed by Kern (1965). All physicochemical parameters are evaluated at a mean film temperature and composition with additional references given in Table 1.

**Table 1. References to Phenomenological Correlations and Physical Constants**

| | References |
|---|---|
| Vapor/liquid thermophysical properties | Reid et al. (1986) |
| Liquid-phase activity coefficients | Hala et al. (1968)<br>Gmehling and Onken (1977) |
| Vapor-phase mass- and heat-transfer coefficients | Colburn and Drew (1937) |
| Liquid-phase mass-transfer coefficients | Palen et al. (1994) |
| Liquid-phase heat-transfer coefficients | Nusselt (1916) |
| Metal thermophysical properties | Perry and Chilton (1973) |

### *Heat transfer*

The composition of the vapors entering the top of the column is $y_V = 0.7$ (methanol). The vapor mixture enters the condenser at the inlet flow rate of $10^4$ g/m$^2$ s, and at a temperature of 370 K. The coolant water enters at the top of the column at 310 K, and the coolant water temperature does not increase by more than 1 K.

The individual resistances (condensate film, inner wall, and cooling water) in the liquid layer can contribute significantly to the overall resistance. Chun and Seban (1972) reported that the thermal resistance of a thick stainless tube is approximately the same order of magnitude as the resistance attributed to the liquid film. Even for low-resistance materials, such as copper tube, the thermal resistance attributed to the wall can significantly affect the overall resistance as the condensate film begins to develop at the inlet of the condenser. Heat flux obtained from the numerical solutions is reported in the form of the ratio, $q/q_o$, where $q_o$ is evaluated assuming negligible heat-transfer resistance in the inner wall and the coolant water; therefore, $q/q_o$ is always less than unity. The available transfer area needed for complete condensation depends on the overall thermal resistance and the thermal gradients. The heat-transfer effects were analyzed over the two domains of the length of the column and the fraction of vapor condensed, but only the former is presented here, in the figures.

Three different cases are considered in Table 2. Heat-transfer coefficients for the inner wall and the coolant water are for Case 1: $h_{\text{wall}} = 207$ kW/m$^2$·K, $h_{cw} = 220$; Case 2: $h_{\text{wall}} = 52$, $h_{cw} = 17$; Case 3: $h_{\text{wall}} = 21$, $h_{cw} = 4$. Case 1 corresponds to negligible thermal resistances, Case 2 to moderate thermal resistances, and Case 3 to high thermal resistances in the inner wall and the coolant water. Table 2 provides other parameters used in the calculations for Cases 1–3. Figure 11

**Table 2. Tabulated Values of the Pertinent Variables Used in the Simulation**

| | Case 1 | Case 2 | Case 3 |
|---|---|---|---|
| *Vapor Phase* | | | |
| $G_{Vo}$ [g/m$^2$·s] | 10,000 | 10,000 | 10,000 |
| $y_{Vo}$ [methanol] | 0.7 | 0.7 | 0.7 |
| $T_{Vo}$ [K] | 370 | 370 | 370 |
| $D_o$ [cm] | 3.5 | 3.5 | 3.5 |
| *Cooling Water/Wall* | | | |
| $T_{CWo}$ [K] | 310 | 310 | 310 |
| $G_{CWo}$ [g/m$^2$·s] | 1E8 | 5E6 | 1E6 |
| $h_{\text{wall}}$ [kJ/m$^2$·s·K] | 207 | 52 | 21 |
| $h_{CW}$ [kJ/m$^2$·s·K] | 220 | 17 | 4 |

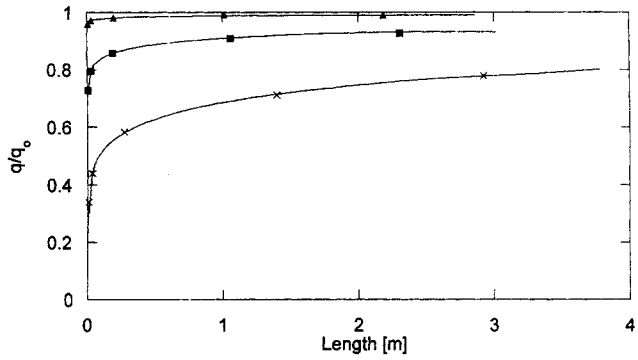


**Figure 11. Effect of wall and cooling water resistances on $q/q_o$ as a function of length for the following three cases described in Table 2 (Case 1 (▲), Case 2 (□), and Case 3 (X)).**

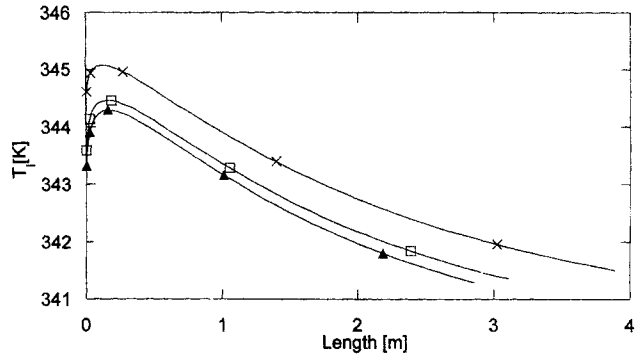


**Figure 12. Interfacial temperature as a function of length for the three cases of Figure 11.**

shows $q/q_o$ as a function of the length. For all the cases considered, $q/q_o$ increases rapidly as the liquid film begins to develop. The thermal resistances in the coolant water and the inner wall dominate the resistance in the condensate film at the inlet of the column. For Case 1 where the thermal resistance in the coolant water and the inner wall is very low, $q/q_o$ stabilizes for tower lengths above 2 m. For Case 3, $q/q_o$ never stabilizes; in fact, the coolant water and the inner wall have considerable control over the liquid resistance even when much of the vapor has condensed. In Case 2, $q/q_o$ stabilizes to a limiting value, but never approaches unity.

Figure 12 shows the interfacial temperature as a function of the length. As noted previously in conjunction with Figure 10 (Case 2), the interfacial temperature first increases anomalously before decreasing with increasing $\zeta$ (Figure 4). This reversal appears to be the result of the liquid-film thickness increasing strongly with $\zeta$ for small values of $\zeta$. Tests show that the reversal is physical and not a numerical artifact. While we have been unable to develop exact equations to explain and predict this reversal, considerable insight into its cause may be gained by considering the three resistances between the interfacial temperature $T_I$ and the cooling water temperature, $T_{cw}$, here assumed constant:

$$q_L = \sum_{i=1}^{C} N_i\left(\overline{H}_i - \overline{h}_i\right) + \Xi_V^* \boldsymbol{h}_V (T_V - T_I)$$

$$= [(T_I - T_{cw})/(R_{cw} + R_w + R_L)], \quad (47)$$

where $R_L = (\delta_L/k_L A_I)$, and $A_I$ is the interfacial area. As assumed by Colburn and Drew (1937), $q_L$ is dominated by the condensation term $w \sum_{i=1}^{C} Z_i(\overline{H}_i - \overline{h}_i)$, whereas the resistances $R_{cw}$ and $R_w$ vary little with $\zeta$. The $\sum_{i=1}^{C} Z_i(\overline{H}_i - \overline{h}_i)$ term also often varies little with $\zeta$, as $Z$ itself is going through a minimum in Figure 13, but the condensation rate falls rapidly near $\zeta = 0$, as shown in Figure 14. Roughly, $(T_I - T_{cw})$ will increase with $\zeta$ whenever the fractional increase in $(R_{cw} + R_w + R_L)$ is more than the fractional decrease in $w$. Results from Nusselt's pure-component model (Eq. 12) are based on assumptions (including constant $T_I$!) that are inconsistent with what we wish to calculate here. Once the initial rise in $T_I$ is accepted, however, other anomalous results such as the dip in $Z$ and $x_L$ in Figure 13 are easily understood.

The overall heat-transfer coefficient for the three cases is shown on Figure 15. The liquid-film heat-transfer coefficient is approximately equal to Case 1, since in this case the heat-transfer resistance is primarily controlled by the liquid film. Figure 15 shows the extent to which the resistance in the wall and coolant water reduces the overall heat-transfer coefficient for Cases 2 and 3 compared to Case 1. Eventually, the condensate film resistance dominates the wall and coolant water resistance.

To check for the effect of the nonideal Ackermann corrections ($\Xi_H^*$) vs. ideal Ackermann corrections ($\Xi_H$), the present three cases were redone assuming the vapor is an ideal gas. Figure 16 shows $[(\Xi_H^*)/(\Xi_H)]$ vs. the fraction of condensed vapor. Deviations from unity at the entrance of the column, where condensation rate is very high, are seen to be significant, especially for Case 1. For low-pressure systems, the effect of nonidealities on the condensation profiles is generally small since the conductive heat flux is only a fraction of the

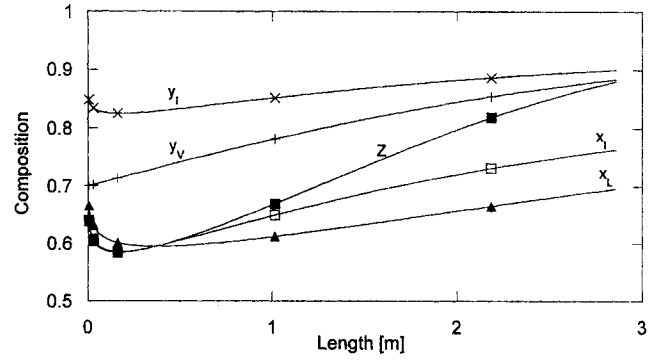


**Figure 13. Composition of bulk vapor (+), interfacial vapor (X), interfacial liquid (□), and bulk liquid (▲), as well as the molar flux fraction of the volatile component (■) for Case 1 described in Table 2.**

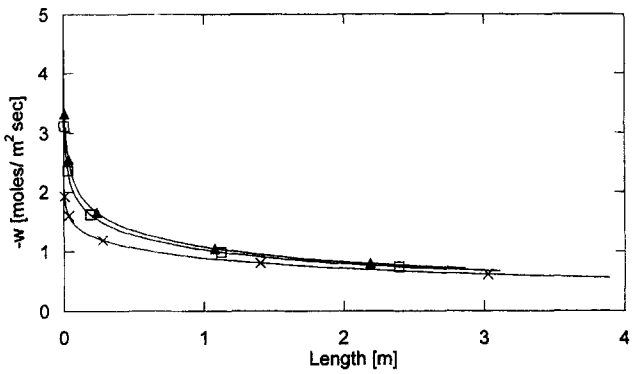


**Figure 14. Net condensation rate $w$ as a function of length for the three cases of Figure 11.**

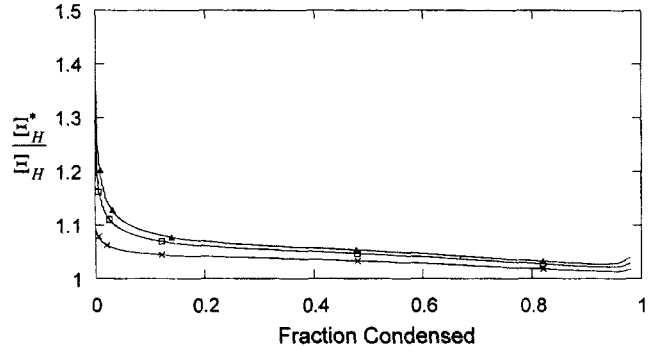


**Figure 16. Ratio of the nonideal correction factor ($\Xi_H^*$) to idealized correction factor ($\Xi_H$) vs. fraction of vapor condensed for the present three cases.**

overall heat flux. As the vapor phase becomes more nonideal, these deviations can become significant. In general, the ideal Ackermann correction factor should be replaced with the nonideal Ackermann correction whenever the components form nonideal solutions, as this correction is easily made within the computer program.

### *Mass transfer*

Figure 13 illustrates the profiles of $y_V$, $y_I$, $x_I$, $x_L$, and $Z$ vs. length for Case 1, while Figure 14 provides the condensation rate $w$ vs. length for all three cases. For cocurrent columns, the dew- and bubble-point curves significantly influence the condensation profiles. This distinction can be seen in Figure 13, which shows the bulk vapor profile, condensing profile, and the condensate profile changing with respect to the dew- and bubble-point curves. The bulk vapor composition increases rapidly since the higher boiling point component, water, is being stripped from the vapor phase to the condensate, also causing the bulk vapor temperature to fall. The bulk vapor profile then approaches the dew-point curve. The condensate profiles, however, show somewhat different behavior than previously assumed. If one assumes that the liquid-phase mass-transfer coefficient is infinity, then the condensate profile should coincide with the bubble-point curve. For the actual case where $k^L$ is finite (nonzero), Figure 13 shows $x_L$ to deviate significantly from $x_I$. The higher the condensation rates, the larger this deviation. The condensing composition $Z$ for cocurrent columns can be characterized by the dew- and bubble-point curves. The condensing composition profile begins at the bubble-point curve, where $x_I$, $x_L$, and $Z$ must begin from a common value at the top of the tower. The interfacial temperature maximization causes the interfacial composition profiles to go through a minimum, which causes the bulk condensate composition and condensing ($Z$) profiles to go through a minimum. The extreme of this minimization is shown best by Case 1, where the condensate composition goes through a significant reversal at $x_L = 0.6$, then rapidly increases. This happens for two reasons. At the inlet of the condenser, the condensate composition is approximately equal to the condensing composition, which is in equilibrium with the dew-point curve. As the interface temperature goes through the maximum, the condensing and bulk condensate profiles turn around sharply. They now follow the generally accepted norm that requires the condensing and the bulk condensate compositions to continuously increase. As the liquid film begins to grow, the condensing composition $Z$ begins to deviate from the bubble-point curve and approaches the dew-point curve. The condensing composition profile terminates at the dew-point curve.

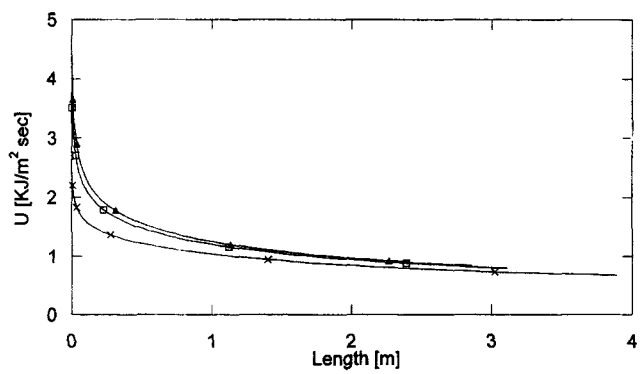


**Figure 15. Overall heat-transfer coefficient, $U$, as a function of length for the three cases of Figure 11.**

Table 3 provides the tower height at which 99% of the inlet vapor is condensed under the conditions given in Cases 1–3, when the liquid mass-transfer coefficient, $k^L$, is taken as (1) infinity–infinitely mixed; (2) zero—no mixing; and (3) fi-

**Table 3. Calculated Length ($\zeta$) of Condenser with 99% of Inlet Vapor Condensed and Relative Error in Assuming the Liquid-Phase Mass-Transfer Coefficient to the Actual Value**

| | Case 1 | Case 2 | Case 3 |
|---|---|---|---|
| $k_L$ = Infinite ($a$) | 2.76 | 3.01 | 3.78 |
| $k_L$ = Finite ($b$) | 2.89 | 3.18 | 3.95 |
| $k_L = 0$ ($c$) | 3.06 | 3.31 | 4.20 |
| Relative error ($b - a$) | 4.50% | 5.35% | 4.30% |
| Relative ($b - c$) | −5.88% | −4.09% | −6.33% |

nite (nonzero) from the correlation of Palen et al. (1994). The first assumption causes the height to be underpredicted by about 5%, while the second assumption leads to overprediction by about the same fraction. The first conclusion is in qualitative agreement with that reached by McNaught (1983).

## Summary

The condensation of mixed vapors is a physically complex topic, requiring an understanding of thermodynamics, heat transfer, and mass transfer. Whether dealing with complete thermodynamic equilibria (CTE), as in our section titled "Thermodynamics and Phase Equilibria," or only with local thermodynamic equilibria (LTE) at the vapor/liquid interface for steady-state wetted-wall tower, as in the rest of the article, we have emphasized the importance of the ratio of molar fluxes at the interface $Z$. The temperature/composition diagram was used to trace both transport phenomena and thermodynamic variables at various tower heights. A selection of possible and impossible sets of temperature and composition profiles was provided. A correction to the Ackermann factor was made, allowing more general use of the design equations when solutions are nonideal.

In the numerical calculations, special emphasis was placed on the liquid phase where the mass transfer is solved without the usual assumptions. It was shown that the interfacial temperature for a methanol/water system goes through a maximum very close to the inlet of the condenser, causing a corresponding minimum in the composition profiles.

## Acknowledgments

The National Science Foundation (Grant CTS-9317812) and the Texas Engineering Experiment Station provided financial support for this work. We acknowledge the technical cooperation of Professor Javier Alvarado and his graduate students at the Department of Chemical Engineering, Technological Institute of Celaya, Mexico. We also thank Professor K. R. Hall and Dean G. P. Peterson of Texas A&M University and personnel of the Heat Transfer Research Institute for technical discussions.

## Notation

$D_{AB}$ = diffusion coefficient, $m^2/s$
$g$ = local gravity, $m/s^2$
$G$ = mass velocity, $g/m^2 \cdot s$
$\Delta \overline{H}$ = change in partial molar enthalpy, J/mole
$J$ = diffusion flux, $mol/m^2 \cdot s$
$L$ = liquid flow rate [moving systems], mol/s
MW = molecular weight
$N_G$ = number of mass-transfer stages
$Re$ = Reynolds number
$Sc$ = Schmidt number
$Z$ = ratio of molar flux of component 1 across the interface to total flux (condensation rate, $w$)

### *Subscripts and superscripts*

1 = inlet
2 = outlet
$i$ = component $i$
$M$ = mass
$P$ = constant pressure
$T$ = constant temperature
$\Gamma$ = latent heat of vaporization
$G$ = vapor phase
$x$ = liquid phase
$\sigma$ = saturation state
$*$ = real state

## Literature Cited

Ackermann, G., "Warmeubergang und Molekulare Stoffubertragung im gleichen Feld bei grossen Temperatur- und Partialdruckdifferenzen," *Ver Deutsch Ing. Forschungshaft*, **382**, 1 (1937).
Bandrowski, J., and A. Kubaczka, "On the Condensation of Multicomponent Vapours in the Presence of Inert Gases," *Int. J. Heat Mass Transf.*, **24**, 147 (1981).
Bell, K. J., and M. A. Ghaly, "An Approximate Generalised Design Method for Multicomponent/Partial Condensers," *AIChE Symp. Ser.*, **69**(131), 72 (1972).
Bett, K. E., J. S. Rowlinson, and G. Saville, *Thermodynamics for Chemical Engineers*, MIT Press, Cambridge, MA (1975).
Bird, R. B., W. E. Stewart, and E. N. Lightfoot, *Transport Phenomena*, Wiley, New York (1960).
Chun, K. R., and R. A. Seban, "Performance Prediction of Falling-Film Evaporators," *J. Heat Transf.*, **94**, 432 (1972).
Colburn, A. P., and T. B. Drew, "The Condensation of Mixed Vapors," *Trans. AIChE*, **33**, 197 (1937).
Colburn, A. P., and O. A. Hougen, "Design of Cooler Condensers for Mixtures of Vapors with Noncondensing Gases," *Ind. Eng. Chem.*, **26**, 1178 (1934).
Denny, V. E., and V. J. Jusionis, "Effects of Forced Flow and Variable Properties on Binary Film Condensation," *Int. J. Heat Mass Transfer*, **15**, 2143 (1972).
Eubank, P. T., E. S. Kim, J. C. Holste, and K. R. Hall, "Effect of Impurities upon Pure Component Thermophysical Properties," *Ind. Eng. Chem. Res.*, **26**, 2020 (1987).
Gmehling, J., and U. Onken, *Vapor Liquid Equilibrium Data Composition: Aqueous-Organic Systems*, DECHEMA Data Ser., Vol. 1, No. 1, Frankfurt, Germany (1977).
Hala, E., Wichterle, I., J. Polak, and T. Boublik, *Vapor-Liquid Equilibrium Data at Normal Pressures*, Pergamon Press, New York (1968).
Kent, E. R., and R. L. Pigford, "Fractionation During Condensation of Vapor Mixtures," *AIChE J.*, **2**, 363 (1956).
Kern, D. Q., *Process Heat Transfer*, McGraw-Hill, New York (1950).
Kreith, F., *Principles of Heat Transfer*, 3rd ed., Intext Press, New York (1973).
Krishna, R., and G. L. Standard, "A Multicomponent Film Model Incorporating an Exact Matrix Method of Solution to the Maxwell-Stefan Equations," *AIChE J.*, **22**, 383 (1976).
Krupiczka, R., A. Rotkegel, K. Oswatitsch, and W. Hantsch, "Selectivity During Condensation of Binary Mixtures in a Nozzle with Countercurrent Flow of Vapour and Condensate," *Chem. Eng. Sci.*, **45**(7), 1685 (1990).
Lewis, W. K., "The Principles of Counter-Current Extraction," *Ind. Eng. Chem.*, **8**, 825 (1916).
Lewis, W. K., and K. C. Chang, "The Mechanism of Rectification," *Trans. AIChE*, **21**, 127 (1928).
Lewis, W. K., and W. G. Whitman, "Principles of Gas Absorption," *Ind. Eng. Chem.*, **16**, 1215 (1924).
McNaught, J. M., "Mass Transfer Correction Terms in Design Methods for Multi-Component Partial Condensers," *Heat Transfer Conf.*, ASME-AIChE, San Diego, p. 111 (1979).
Nusselt, W. Z., "Die Oberflachenkondensation des Wasserdampfes," *Ver. Deut. Ing.*, **60**, 541 (1916).
Othmer, D. F., "The Condensation of Steam," *Ind. Eng. Chem.*, **21**, 577 (1929).
Palen, J. W., Q. Wang, and J. C. Chen, "Falling Film Evaporation of Binary Mixtures," *AIChE J.*, **40**(2), 207 (1994).
Perry, R. H., and C. H. Chilton, *Chemical Engineers' Handbook*, 5th ed., McGraw-Hill, New York (1973).
Pratt, H. R. C., and P. G. Tuohey, "Binary and Multicomponent Mass Transfer at 'High Transfer Rates'," *Chem. Eng. J.*, **18**, 251 (1979).
Reid, R. C., J. M. Prausnitz, and B. E. Poling, *The Properties of Gases & Liquids*, 4th ed., McGraw-Hill, New York (1986).
Schrodt, J. T., and E. R. Gerhard, "Simultaneous Condensation of Methanol and Water from a Noncondensing Gas on Vertical Tubes in a Bank," *Ind. Eng. Chem. Fundam.*, **7**, 281 (1968).

Silver, L., "Gas Cooling with Aqueous Condensation," *Trans. Inst. Chem. Eng.*, **25**, 30 (1947).
Slattery, J. C., *Momentum, Energy, and Mass Transfer in Continua*, McGraw-Hill, New York (1972).
Smith, J. M., H. C. Van Ness, and M. M. Abbott, *Introduction to Chemical Engineering Thermodynamics*, 5th ed., McGraw-Hill, New York (1996).
Sparrow, E. M., and E. Marschall, "Binary Gravity-Flow Film Condensation," *J. Heat Transfer*, **91**, 205 (1969).
Stewart, W. E., and R. Prober, "Matrix Calculation of Multicomponent Mass Transfer in Isothermal Systems," *Ind. Eng. Chem. Fundam.*, **3**, 224 (1964).
Strickland-Constable, R. F., "Two Phase Equilibrium in Binary and Ternary Systems," *Proc. Roy. Soc.*, **A209**, 14 (1951).
Taylor, R., and L. W. Smith, "On Some Explicit Approximate Solutions of the Maxwell-Stefan Equations for the Multicomponent Film Model," *Chem. Eng. Commun.*, **14**, 361 (1982).
Taylor, R., and R. Krishna, *Multicomponent Mass Transfer*, Wiley, New York (1993).
Toor, H. L., "Diffusion in Three Component Gas Mixtures," *AIChE J.*, **3**, 198 (1957).
Treybal, R. E., *Mass-Transfer Operations*, 3rd ed., McGraw-Hill, New York (1980).
Van Es, J. P., and P. M. Heertjes, "The Condensation of a Vapor of a Binary Mixture," *Brit. Chem. Eng.*, **7**(8), 580 (1962).
Webb, D. R., M. Fahrner, and R. Schwaab, "The Relationship Between the Colburn and Silver Methods of Condenser Design," *Int. J. Heat Mass Transf.*, **39**, 3147 (1996).

*Manuscript received Dec. 11, 1997, and revision received Aug. 24, 1998.*